min. The mixture was slowly warmed to room temperature and then stirred for 15 h. The solvent was evaporated in vacuo and the residue was triturated with cyclohexane (3 × 75 mL) and filtered. The solvent was removed under reduced pressure to afford 0.45 g (98%) of the crude azirine. IR and NMR of this material were consistent with those reported above and the isolated material was of sufficient purity to be used directly.

Acknowledgment. Support of this work by the National Science Foundation, Alfred P. Sloan Foundation, and the Camille and Henry Dreyfus Teacher Scholar Program is greatly appreciated by M.S.P. Special thanks are due to B. B. Wright for a sample of azirine **16**, to S. E. Sugamori for technical assistance, and to Professor K. Horn for the communication of unpublished results.

Registry No. 1, 10378-55-9; **4**, 64833-56-3; **8**, 66-77-3; **13**, 70840-50-5; **14**, 102421-45-4; **15**, 86602-71-3; **16**, 88235-59-0; **17Z**, 88226-29-3; **17E**, 88226-30-6; **18Z**, 88226-31-7; **18E**, 88226-32-8; acrylonitrile, 107-13-1; 1-acetonaphthone tosylhydrazone, 102421-44-3; 8-methylnaphthaldehyde tosylhydrazone, 102421-46-5; cyclohexyl chloride, 542-18-7; (1-naphthyl)cyclohexylmethanol, 94823-85-5; 1-bromonaphthalene, 90-11-9; propylene oxide, 75-56-9; 1-(1-naphthyl)-2-propanol, 27653-13-0; 1-(1-naphthyl)-2-propanone, 33744-50-2; 1,1-dimethylhydrazine, 57-14-7; (*Z*)-1-(1-naphthyl)-2-propanone *N,N*-dimethylhydrazone, 102421-47-6; (*E*)-1-(1-naphthyl)-2-propane *N,N*-dimethylhydrazone, 102421-48-7; (*Z*)-1-(1-naphthyl)-2-propane trimethylhydrazonium iodide, 102421-49-8; (*E*)-1-(1-naphthyl)-2-propane trimethylhydrazonium iodide, 102421-50-1; (*Z*)-1-(1-naphthyl)-2-propanone oxime, 20557-52-2; (*E*)-1-(1-naphthyl)-2-propanone oxime, 19534-15-7; (*Z*)-1-(1-naphthyl)-2-propanone *p*-nitrobenzoyloxime, 102421-51-2; (*E*)-1-(1-naphthyl)-2-propanone *p*-nitrobenzoyloxime, 102421-52-3; *p*-nitrobenzoyl chloride, 122-04-3; cyclohexane, 110-82-7; cyclopentane, 287-92-3; methylcyclopentane, 108-87-2; methanol, 67-56-1; oxygen, 7782-44-7; 2,3-dimethyl-2-butene, 563-79-1; 2,5-dimethyl-2,4-hexadiene, 764-13-6; *cis*-1,2-dichloroethylene, 156-59-2; *trans*-1,2-dichloroethylene, 156-60-5; *tert*-butyl alcohol, 75-65-0; diethyl fumarate, 623-91-6.

He I Photoelectron Spectra, Valence Electronic Structure, and Back Bonding in the Deltahedral Boron Chlorides, B_4Cl_4, B_8Cl_8, and B_9Cl_9

P. R. LeBreton,* S. Urano, M. Shahbaz, S. L. Emery, and J. A. Morrison*

Contribution from the Department of Chemistry, University of Illinois at Chicago, Chicago, Illinois 60680. *Received August 30, 1985*

Abstract: He I photoelectron spectra have been obtained for B_4Cl_4, B_8Cl_8, and B_9Cl_9, the three boron monohalides which have been structurally characterized. The 6 photoelectron bands arising from the 15 highest occupied molecular orbitals of B_4Cl_4 are clearly resolved, but the presence of a seventh band at 19.51 eV, which had been previously assigned to the $2a_1$ orbital of B_4Cl_4, is not confirmed. The spectra of B_8Cl_8 and B_9Cl_9 are much more complex and less resolved than that of B_4Cl_4. Rather than discrete bands, four broad envelopes of photoelectron activity are found. GAUSSIAN 80 (STO-3G) ab initio calculations on B_4Cl_4 and B_8Cl_8 and INDO semiemperical calculations on B_4Cl_4, B_8Cl_8, and B_9Cl_9 demonstrate that the four envelopes result from four different types of molecular orbitals. Each type is distinguished by characteristic boron and chlorine contributions to the molecular wave function. Comparison of the ab initio and semiemperical results indicates that they are in remarkably good agreement in the assignment of the B_8Cl_8 spectral data. Back bonding in the polynuclear boron chlorides is shown to be much more complex than in smaller molecules like BCl_3. The stability of the neutral boron chlorides (which have only $2n$ framework electrons) is found to be one of the results of the differences between the makeup of the HOMO orbitals of the polyhedral boron chlorides and that of the analogous boron hydrides. The average boron–boron overlap populations were examined using the results from both types of calculation. For a series of eight boron chloride structures the average boron–boron overlap population decreases in the order $B_9Cl_9^{2-} > B_9Cl_9 > B_8Cl_8^{2-} > B_8Cl_8 > B_4Cl_4$ (T_d) > B_4Cl_4 (D_{4h}) > B_2Cl_4 (D_{2d}) > B_2Cl_4 (D_{2h}). Except for B_8Cl_8, the core overlap populations correlate well with the experimental thermal stability data where the latter are available.

The polyhedral boron chlorides are a family of volatile cluster compounds which are related in that they have the common molecular formula B_nCl_n. The species for which $n = 4$ and 8–12 have been relatively well characterized,[1,2] and the existence of the compounds where $n = 13$–20 has been indicated by mass spectrometry.[3] The structures of only three of the boron monochlorides, B_4Cl_4, B_8Cl_8, and B_9Cl_9, have been determined by crystallographic studies; all three have been found to have closo geometries.

Octaboron octachloride and nonaboron nonachloride are of interest because they are prototypical electron-deficient clusters, clusters which—to the extent that ligand-to-cage bonding can be factored from intracage interactions—possess only $2n$ framework electrons. This is two fewer than the number ($2n + 2$, $n \neq 4$) most frequently observed in n-vertex *closo*-boranes, -carboranes, -metalloboranes, and -metal carbonyl clusters.[4,5] The latter number, $2n + 2$, has been referred to as the "magic" number of electrons,[6] the number which gives rise to superaromatic bonding.[7] Similarly, the smallest cluster in the series, B_4Cl_4, can also be considered to be electron deficient since there are only 8 framework

(1) Davan, T.; Morrison, J. A. *Inorg. Chem.* **1979**, *18*, 3194.
(2) Davan, T. Ph.D. Thesis, University of Illinois, Chicago, 1982. Davan, T.; Morrison, J. A. *Inorg. Chem.*, in press.
(3) Saulys, D. A.; Kutz, N. A.; Morrison, J. A. *Inorg. Chem.* **1983**, *22*, 1821.
(4) O'Neill, M. E.; Wade, K. In *Metal Interactions with Boron Clusters*; Grimes, R. N., Ed.; Plenum: New York, 1982. Mingos, D. M. P. *Acc. Chem. Res.* **1984**, *17*, 311.
(5) Stone, A. J. *Inorg. Chem.* **1981**, *20*, 563. King, R. B.; Rouvray, D. H. *J. Am. Chem. Soc.* **1977**, *99*, 7834. Teo, B. K.; Longoni, G.; Chung, F. R. K. *Inorg. Chem.* **1984**, *23*, 1257. Lipscomb, W. N. *Inorg. Chem.* **1979**, *18*, 2328. Epstein, I. R.; Lipscomb, W. N. *Inorg. Chem.* **1971**, *10*, 1921.
(6) Rudolph, R. W. *Acc. Chem. Res.* **1976**, *9*, 446.
(7) Hall, J. H., Jr.; Epstein, I. R.; Lipscomb, W. N. *Inorg. Chem.* **1973**, *12*, 915. Bicerano, J.; Marynick, D. S.; Lipscomb, W. N. *Inorg. Chem.* **1978**, *17*, 3443. Chari, S. L.; Chiang, S.; Jones, M., Jr. *J. Am. Chem. Soc.* **1982**, *104*, 3138. Jemmis, E. D.; Schleyer, P. v. R. *J. Am. Chem. Soc.* **1982**, *104*, 4781.

0002-7863/86/1508-3937$01.50/0

electrons in this compound rather than the 12 electrons almost universally found in tetrahedral cage species. While other clusters with $2n$ framework electron counts have been prepared, the advantage of the polyhedral boron halides discussed here is that they form the only complete series of homoleptic, homonuclear cage compounds, all of which contain $2n$ framework electrons.

One of the most interesting questions in this area of chemistry is why is it that the $2n$ framework electron chlorides B_nCl_n are readily formed when the analogous hydrides, compounds like B_8H_8 or B_9H_9, have not been reported? That is, what feature of the bonding is responsible for the fact that the neutral halogen-substituted compounds appear to be much more stable than the neutral hydrides?

Several studies have shown that even though they do not contain $2n + 2$ framework electrons, the boron monochlorides are of reasonable thermal stability. For example, the 9-atom cage compound, B_9Cl_9, decomposes only very slowly in BCl_3, even at 400 °C.[2] The smallest cluster, B_4Cl_4, has been found to be more thermally stable than both *C*,3-$(CH_3)_2C_2B_3H_3$ and 1,5-$C_2B_3H_5$, the $2n + 2$ framework electron cage compounds nearest in size.[1] In his earlier study, Muetterties was unable to determine whether the neutral cluster, HB_9Cl_8, or the reduced ion, $HB_9Cl_8^{2-}$, was the thermodynamically favored aggregate.[8]

The observed stability of the $2n$ framework electron polyhedral boron chlorides has been widely attributed to halogen-to-cage back bonding. This interaction has been postulated to enhance the bond strengths in these compounds by delocalizing chlorine lone-pair electron density to the boron atoms of the cage by means of the molecular orbitals of the appropriate symmetry.[6,9-16] In B_4Cl_4, for example, the 1e orbitals have been specified as the pertinent back-bonding orbitals. This explanation, however, fails to explain several experimental results. For instance, $(t\text{-Bu})_4B_4$, a compound in which back-bonding effects would be expected to be minimal, is readily synthesized,[17] whereas, perhaps fortuitously, no experimental routes are currently known for the preparation of B_4F_4 or B_4Br_4, species in which significant back bonding might be expected.[18,19] The fact that B_9I_9 exists has been taken to imply that the B_9 core in that compound is stabilized by back-donation from the halide ligands,[12] yet the synthesis of $B_9(t\text{-Bu})_9$[20] is an indication that while halide ligands may be advantageous in the nine-atom system, they are not required.

Although there has been considerable interest in the molecular geometries and the bonding of the boron monohalides, their electronic structures have not been extensively probed experimentally. UV–vis studies have been reported for B_4Cl_4,[13] B_8Cl_8,[21] and B_9Cl_9,[22] but photoelectron[14] and molecular orbital calculations at the semiemperical or ab initio levels have been restricted to B_4Cl_4.[15,16,23]

Recent work in one of our laboratories has employed UV photoelectron spectroscopy to investigate the electronic structures of molecules of increasing size and complexity.[24-27] These studies have been greatly aided by the availability of the expanded ab initio and semiemperical molecular orbital computational methods which are necessary for the interpretation of the spectroscopic data.[24-28]

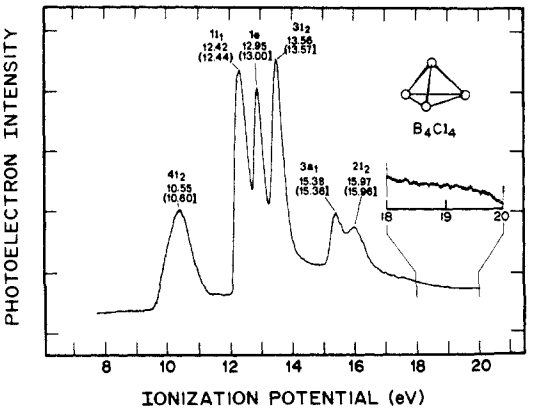

Figure 1. He I photoelectron spectrum and assignments for B_4Cl_4. Previous values in parentheses. The inset sensitivity is 10X that of the full spectrum.

The objectives of the present study were to obtain the He I photoelectron spectra of B_4Cl_4, B_8Cl_8, and B_9Cl_9, the only three boron monochlorides of known structure, and to then interpret these results with the aid of ab initio [GAUSSIAN 80 (STO-3G)][29] and semiemperical [enlarged and spectroscopically parameterized version of INDO][30] molecular orbital calculations. The size limitation of the available GAUSSIAN 80 program restricts the use of the STO-3G all electron calculations to B_4Cl_4 and B_8Cl_8, whereas the INDO program is capable of treating all three of the cluster compounds. Furthermore, INDO calculations include chlorine 3d orbitals in the basis set. It has been previously suggested that these orbitals may contribute significantly to some of the B_4Cl_4 molecular orbitals.[13,15] The ab initio basis set is minimal and does not contain Cl 3d orbitals.

The He I photoelectron spectrum of B_4Cl_4 has been reported previously;[14] however, one feature of that spectrum was unusual enough to suggest a reexamination. In the PES of B_4Cl_4, five intense bands, one of which was composite, were observed with ionization potentials from 10.6 to 16.0 eV. A sixth band was detected at 19.51 eV and assigned to the $2a_1$ orbital.[14] Later, two separate ab initio studies of B_4Cl_4 were able to calculate the ionization potentials of the first five bands to within 9%[15] and (after scaling) 7%,[16] but each calculation indicated that the ionization potential of the sixth band should be substantially in excess of 21.2 eV, the energy of the He I emission line.

Experimental Section

Preparation of the Polyhedral Boron Chlorides. Air and moisture were excluded by means of standard vacuum line and glovebox techniques. Tetraboron tetrachloride was synthesized from the radio frequency discharge of BCl_3.[1] Octaboron octachloride was prepared from the thermal reaction of B_2Cl_4 in CCl_4 at 100 °C.[20] Nonaboron nonachloride was isolated from the decomposition of B_2Cl_4 at 450 °C.[2] The purity of the samples was routinely assessed by boron NMR spectroscopy and mass spectrometry. Except for a small amount (<3%) of B_9Cl_9 which was present in the B_8Cl_8 sample, no contaminants were observed.

(8) Muetterties, E. L. In *Boron Hydride Chemistry*; Muetterties, E. L., Ed.; Academic: New York, 1975; p 10.
(9) Longuet-Higgens, H. C. *Q. Rev.*, **1957**, *11*, 121.
(10) Lipscomb, W. N. *Boron Hydrides*; W. A. Benjamin: New York, 1963; p 89.
(11) Kaczmarczyk, A.; Kolski, G. B. *Inorg. Chem.* **1965**, *4*, 665.
(12) Wong, E. H. *Inorg. Chem.* **1981**, *20*, 1300.
(13) Massey, A. G.; Urch, D. S. *J. Chem. Soc.* **1965**, 6180.
(14) Lloyd, D. R.; Lynaugh, N. *J. Chem. Soc., Chem. Commun.* **1971**, 627.
(15) Hall, J. H.; Lipscomb, W. N. *Inorg. Chem.* **1974**, *13*, 710.
(16) Guest, M. F.; Hiller, I. H. *J. Chem. Soc., Faraday Trans. 2* **1974**, *70*, 398.
(17) Davan, T.; Morrison, J. A. *J. Chem. Soc., Chem. Commun.* **1981**, 250.
(18) Timms, P. L. *Acc. Chem. Res.* **1973**, *6*, 118.
(19) Massey, A. G. *Adv. Inorg. Chem. Radiochem.* **1983**, *26*, 1.
(20) Emery, S. L.; Morrison, J. A. *J. Am. Chem. Soc.* **1982**, *104*, 6790.
(21) Lanthier, G. F.; Kane, J.; Massey, A. G. *J. Inorg. Nucl. Chem.* **1971**, *33*, 1569.
(22) Lanthier, G. F.; Massey, A. G. *J. Inorg. Nucl. Chem.* **1970**, *32*, 1807.
(23) Armstrong, D. R.; Perkins, P. G.; Stewart, J. J. *J. Chem. Soc. A* **1971** 3674.
(24) Lin, J.; Yu, C.; Peng, S.; Akiyama, I.; Li, K.; Lee, L. K.; LeBreton, P. R. *J. Am. Chem. Soc.* **1980**, *102*, 4627.
(25) Yu, C.; O'Donnell, T. J.; LeBreton, P. R. *J. Phys. Chem.* **1981**, *85*, 3851.
(26) Shahbaz, M.; Urano, S.; LeBreton, P. R.; Rossman, M. A.; Hosmane, R. S.; Leonard, N. J. *J. Am. Chem. Soc.* **1984**, *106*, 2805.
(27) Rossman, M. A.; Leonard, N. J.; Urano, S.; LeBreton, P. R. *J. Am. Chem. Soc.* **1985**, *107*, 3884.
(28) Lee, L. K.; Sabelli, N. H.; LeBreton, P. R. *J. Phys. Chem.* **1982**, *86*, 3926.
(29) The GAUSSIAN 80 program was obtained from the Quantum Chemistry Program Exchange at the University of Indiana.
(30) Ridley, J. E.; Zerner, M. C. *Theor. Chim. Acta* **1973**, *32*, 111. Ridley, J. E.; Zerner, M. C. *Theor. Chim. Acta* **1976**, *42*, 223. Bacon, A. D.; Zerner, M. C. *Theor. Chim. Acta* **1979**, *53*, 21. Zerner, M. C.; Loew, G. H.; Kirchner, R. F.; Mueller-Westerhoff, U. T. *J. Am. Chem. Soc.* **1980**, *102*, 589.

Table I. STO-3G and INDO Population Analyses and Ionization Potentials of B_4Cl_4[a]

orbital	% B 2s	% B 2p	% Cl 3s	% Cl 3p	ionization potential, eV
$4t_2$	12.1 (1.9)	25.4 (15.7)	0.0 (0.0)	57.6 (81.4)	9.663 (12.388)
$1t_1$	0.0 (0.0)	2.5 (0.8)	0.0 (0.0)	90.8 (99.3)	12.483 (13.513)
1e	0.0 (0.0)	6.0 (12.6)	0.0 (0.0)	87.5 (86.7)	12.973 (14.350)
$3t_2$	0.0 (0.6)	22.5 (26.0)	3.0 (7.8)	69.1 (64.7)	13.851 (15.551)
$3a_1$	5.1 (4.8)	16.4 (14.5)	20.0 (18.9)	52.8 (61.2)	15.368 (16.360)
$2t_2$	21.8 (14.8)	10.5 (44.8)	20.4 (20.0)	39.8 (17.8)	16.337 (19.456)

[a] Only molecular orbitals observed by He(I) spectroscopy included; numbering begins with the valence orbitals. Results from ab initio calculations are given without parentheses. Results from INDO calculations are given in parentheses.

Determination of the Spectra. The He I photoelectron spectra were obtained with a Perkin-Elmer PS-18 spectrometer. Samples of B_4Cl_4 were introduced through a gas probe, while B_8Cl_8 and B_9Cl_9 were introduced through a heated solids probe at 44 and 58 °C, respectively. The latter two compounds were volatilized from 4-mm Pyrex tubes which were sealed until just prior to insertion into the spectrometer.

Spectra from at least three separate preparations of each compound were obtained and calibrated to the $^2P_{1/2}$ and $^2P_{3/2}$ ionic states of xenon and argon. Additionally, the spectrum recorded 5 hours after the introduction of each sample was compared to that obtained after 30 min. No changes in either the position or relative band intensities were observed. However, small amounts of boron trichloride, characterized by a very intense band at 12.7 eV, were present immediately after the initial introduction of B_8Cl_8 and B_9Cl_9. As a test of the spectrometer sensitivity in the 19–20-eV region, the spectrum of *p*-dioxane was examined; the 19.4-eV band of this compound was clearly evident.[31]

Molecular Orbital Calculations. Calculations were carried out on the boron chlorides B_2Cl_4, B_4Cl_4, B_8Cl_8, $B_8Cl_8^{2-}$, B_9Cl_9, and $B_9Cl_9^{2-}$. The bond angles and bond lengths used for B_2Cl_4 were taken from the crystallographic data.[32] However, D_{2d} symmetry (which is consistent with gas-phase Raman and IR studies[33]) was employed in the B_2Cl_4 calculation in addition to the D_{2h} structure found in the solid state. In the gas phase B_4Cl_4 was assumed to be tetrahedral with boron–boron and boron–chloride distances of 1.70 Å.[34,35] The structural data for dodecahedral B_8Cl_8 were obtained from the literature.[36,37] For B_9Cl_9, point group D_{3h}, the published data[38] are incomplete since the angle between the six equivalent BCl bonds and the 3-fold axis as well as the prism height is unreported. The present calculations are based upon an angle of 135° and a prism height of 2.08 Å.[39] Crystallographic data are not available for the dianions; unless otherwise noted the geometries employed were those of the corresponding neutral compounds.

Results

Spectroscopic Results. The He I photoelectron spectrum of B_4Cl_4 obtained in this study is shown in Figure 1. The measured ionization potentials are given above each band along with those previously reported, the latter being enclosed in parentheses. The spectrum in Figure 1 is similar to that previously observed; however, there are two differences. First, relative to the band at 10.55 eV, the bands of higher ionization potential, 15.38 and 15.97 eV, are slightly more intense in the present spectrum than in that previously published. Second, there is no evidence for a weak band centered at 19.51 eV. The inset in Figure 1 results from a 10-fold increase in sensitivity in the 18–20-eV region, see ref 14.

The photoelectron spectra of B_8Cl_8 and B_9Cl_9 are presented in Figures 2 and 3, respectively. While the individual spectra do differ in detail, there are evident similarities within the series. For example, in each case the band or envelope of bands with the lowest ionization potential is centered at 10.6 (±0.1) eV. Similarly, the bands arising from the orbitals with the highest observed ionization potentials appear as broad envelopes at 15.7 (±0.3) eV. The remaining, intermediate energy bands are the most intense and the most complex in the spectra. In all three spectra there is a very strong band or envelope of bands at 12.3 (±0.15) eV accompanied by other bands that are centered in the 13–14-eV energy region.

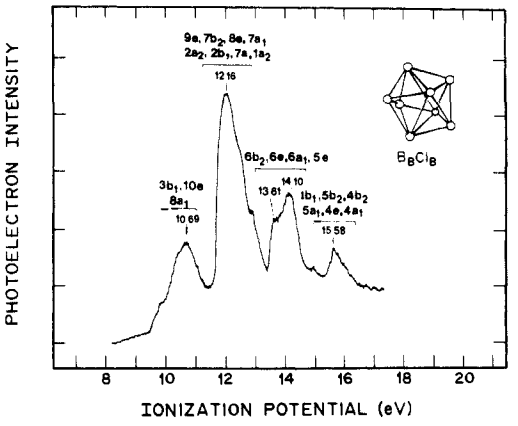

Figure 2. He I photoelectron spectrum and assignments for B_8Cl_8.

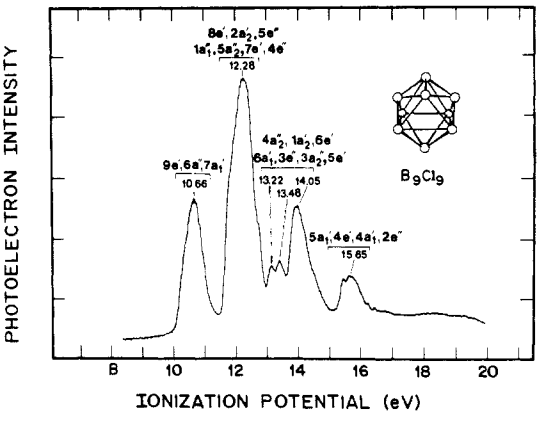

Figure 3. He I photoelectron spectrum and assignments for B_9Cl_9.

Computational Results. Population Analyses. Tables I and II contain the atomic contributions to the molecular orbitals from both the ab initio and the INDO calculations on B_4Cl_4 and B_8Cl_8. The INDO results from B_9Cl_9 are found in Table III. For B_4Cl_4 and B_8Cl_8 the trends within each of the data sets are in excellent agreement. With the exception of the $1b_1$ orbital of B_8Cl_8 the largest differences in the character of the orbitals predicted by the two calculations are found in the highest occupied molecular orbitals and in the most strongly bound orbitals in the spectra. The ab initio results predict significantly higher boron contributions in the orbitals in the HOMO region than the INDO calculations do. They also suggest that the orbitals deeper in energy ($2t_2$ for B_4Cl_4, 4e and $4a_1$ of B_8Cl_8) contain more B 2s and Cl 3p character than that indicated by the INDO calculations.

A comparison of the population analyses for the remaining orbitals indicates that the trends obtained from each of the cal-

(31) Kimura, K.; Katsumata, S.; Achiba, Y.; Yamazaki, T.; Iwata, S. *Handbook of HeI Photoelectron Spectra of Fundamental Organic Molecules*; Halsted: New York, 1981; p 207.
(32) Atoji, M.; Wheatley, P. J.; Lipscomb, W. N. *J. Chem. Phys.* **1957**, *27*, 196.
(33) Linevsky, M. J.; Shull, E. R.; Mann, D. E.; Wartik, T. *J. Am. Chem. Soc.* **1953**, *75*, 3287. Ryan, R. R.; Hedberg, K. *J. Chem. Phys.* **1969**, *50*, 4986.
(34) Atoji, M.; Lipscomb, W. N. *Acta Crystallogr.* **1953**, *6*, 547.
(35) Brown, F. R.; Miller, F. A.; Sourisseau, C. *Spectrochim. Acta, Part A* **1976**, *32A*, 125.
(36) Jacobson, R. A.; Lipscomb, W. N. *J. Chem. Phys.* **1959**, *31*, 605.
(37) Pawley, G. S. *Acta Crystallogr.* **1966**, *20*, 631.
(38) Hursthouse, M. B.; Kane, J.; Massey, A. G. *Nature (London)* **1970**, *228*, 659.
(39) O'Neill, M. E.; Wade, K. *Inorg. Chem.* **1982**, *21*, 461.

Table II. STO-3G and INDO Population Analyses and Ionization Potentials of B_8Cl_8[a]

orbital	% B 2s	% B 2p	% Cl 3s	% Cl 3p	ionization potential, eV
$3b_1$	0.0 (0.0)	31.7 (13.0)	0.0 (0.0)	63.8 (85.9)	9.631 (12.665)
10e	5.2 (0.7)	21.7 (13.6)	0.0 (0.0)	67.9 (84.6)	10.504 (12.635)
$8a_1$	4.7 (0.4)	20.6 (12.4)	0.0 (0.0)	69.5 (86.3)	10.581 (12.557)
9e	3.7 (0.4)	5.5 (2.1)	0.3 (0.0)	83.9 (97.3)	12.237 (13.395)
$7b_2$	1.6 (0.3)	1.1 (0.1)	0.0 (0.0)	90.5 (99.5)	12.292 (13.368)
8e	0.1 (0.2)	2.4 (2.3)	0.0 (0.1)	90.9 (97.4)	12.443 (13.429)
$7a_1$	0.0 (0.0)	2.7 (0.6)	0.0 (0.0)	90.5 (99.2)	12.506 (13.408)
$2a_2$	0.0 (0.0)	2.3 (0.2)	0.0 (0.0)	91.0 (99.8)	12.656 (13.702)
$2b_1$	0.0 (0.0)	2.7 (0.6)	0.0 (0.0)	90.6 (99.4)	12.856 (13.797)
7e	0.3 (0.0)	3.1 (1.0)	0.0 (0.0)	90.0 (98.9)	12.956 (13.815)
$1a_2$	0.0 (0.0)	5.7 (6.0)	0.0 (0.0)	87.8 (93.7)	13.468 (14.316)
$6b_2$	1.2 (1.0)	10.8 (17.5)	1.0 (2.4)	80.8 (78.1)	14.086 (15.148)
6e	1.1 (0.7)	23.1 (22.4)	10.2 (7.4)	60.1 (68.9)	14.345 (15.310)
$6a_1$	4.9 (3.2)	16.7 (16.7)	10.4 (9.9)	62.0 (69.3)	14.860 (15.882)
5e	1.8 (2.2)	23.2 (20.3)	7.6 (9.2)	62.2 (67.6)	14.897 (15.827)
$1b_1$	0.0 (0.0)	42.0 (82.0)	0.0 (0.0)	53.8 (14.1)	15.393 (20.565)
$5b_2$	2.3 (1.5)	22.6 (20.6)	17.3 (12.3)	52.4 (65.3)	15.536 (16.113)
$4b_2$	15.9 (6.5)	9.6 (24.8)	20.7 (21.8)	46.9 (45.2)	16.077 (17.804)
$5a_1$	7.2 (6.2)	20.0 (13.9)	23.5 (32.0)	44.0 (47.1)	16.410 (17.820)
4e	20.6 (6.0)	23.7 (59.9)	14.4 (17.3)	35.1 (13.7)	17.026 (21.000)
$4a_1$	19.4 (3.4)	28.4 (59.4)	16.0 (24.6)	32.8 (9.8)	17.469 (22.424)

[a] Only orbitals observed by He(I) spectroscopy included; numbering begins with the valence orbitals. Results from INDO calculations given in parentheses. Orbitals are listed in order of increasing ionization potential as predicted by the ab initio calculations.

Table III. INDO Population Analysis and Ionization Potentials of B_9Cl_9[a,b]

orbital	% B 2s	% B 2p	% Cl 3s	% Cl 3p	ionization potential, eV
9e′	0.5	12.9	0.0	85.7	12.630
6e″	0.3	12.6	0.0	86.1	12.729
$7a_1'$	0.4	9.8	0.0	89.1	12.804
8e′	0.3	0.5	0.0	99.1	13.500
$2a_2'$	0.0	0.1	0.0	99.9	13.523
5e″	0.0	0.3	0.0	99.6	13.604
$1a_1''$	0.0	0.6	0.0	99.4	13.632
$5a_2''$	0.4	1.1	0.0	98.4	13.638
7e′	0.0	0.5	0.0	99.4	13.668
4e″	0.0	1.0	0.0	98.9	13.799
$4a_2''$	0.0	10.2	0.8	88.7	14.508
$1a_2'$	0.0	26.4	0.0	72.0	15.480
6e′	1.9	20.1	9.3	68.1	15.683
$6a_1'$	2.6	19.4	9.2	68.1	15.788
3e″	3.7	17.7	10.5	67.2	15.922
$3a_2''$	0.8	25.6	9.6	63.2	15.978
5e′	1.3	21.5	10.1	66.5	15.988
$5a_1'$	6.7	12.4	36.8	43.4	18.248
4e′	4.7	58.0	23.7	10.9	21.832
$4a_1'$	4.0	62.9	21.5	8.9	22.225
2e″	3.1	57.9	26.2	10.0	22.302

[a] Only orbitals observed by He(I) spectroscopy included; numbering begins with the valence orbitals. [b] Prism height, 2.08 Å; angle between the six equivalent BCl bonds (prism B–Cl) and C_3 axis, 135°.

culations are very similar. Even the absolute values correspond quite well (to within 14%). The close agreement between the results from the two types of treatment for B_4Cl_4 and B_8Cl_8 is supportive of the trends in the B_9Cl_9 INDO population analysis found in Table III.

Participation of Inner-Shell and Chlorine 3d Atomic Orbitals. Tables I–III contain only the contributions of the boron and chlorine valence orbitals. The inner-shell contributions to the molecular orbitals examined here are small. The largest B 1s contribution indicated by the STO-3G calculations is 2.4% in the 4e orbitals of B_8Cl_8. The maximum Cl 2p content is 6.8% which is found in the $1t_1$ orbitals of B_4Cl_4. The Cl 1s and 2s character is less than 1% in all orbitals.

The amounts of Cl 3d participation obtained from the INDO calculations are also small, generally less than 2%. Overall, the largest amount of Cl 3d character, 3.9%, is found in the $1b_1$ orbital of B_8Cl_8. The Cl 3d contribution to the 1e orbitals of B_4Cl_4 is 0.7%.

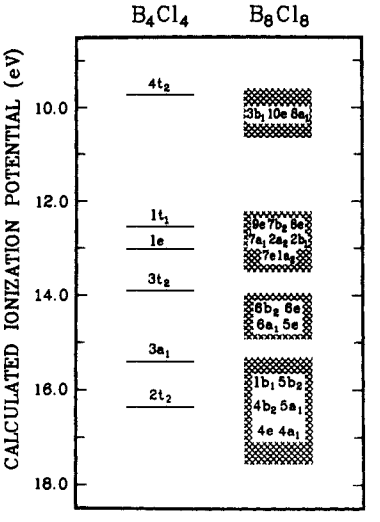

Figure 4. Ab initio energy level diagrams for B_4Cl_4 and B_8Cl_8.

Ionization Potentials. Theoretical ionization potentials were obtained by the application of Koopmans' theorem[40] to the results of the ab initio and the INDO calculations. They are listed in Tables I–III. The patterns of photoelectron intensity predicted by the STO-3G and INDO treatments are presented in Figures 4 and 5, respectively.

Assignment of the B_4Cl_4 Spectrum. For B_4Cl_4, except for the $4t_2$ orbitals for which the calculated ionization potentials are 0.89 eV (8.4%) lower than observed, the absolute ionization potentials from the ab initio calculations are all within 0.4 eV (2.3%) of those obtained from the experimental spectrum, Figure 1. The present ab initio results are also in good agreement with those previously obtained from both Gaussian-1[6] and Slater-type[15] basis functions. Like the previous calculations, they indicate that the ionization potential of the $2a_1$ orbital (25.1 eV) is too large for that orbital to be observed in the He(I) spectrum.

When compared with experiment, the B_4Cl_4 INDO results are less accurate. The calculated ionization potentials are uniformly 1.0–2.0 eV larger than the experimental values, except for the $2t_2$ orbitals which are predicted to be 3.5 eV larger than measured.

(40) Koopmans, T. *Physica* **1934**, *1*, 104.

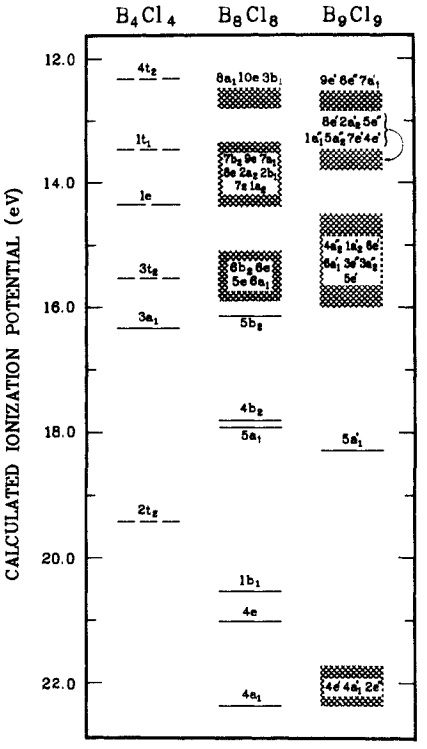

Figure 5. INDO energy level diagrams for B_4Cl_4, B_8Cl_8, and B_9Cl_9.

The result is that the calculated difference between the $3a_1$ and the $2t_2$ orbitals (3.1 eV) is much greater than obtained from the spectrum (0.6 eV). Similarly, the predicted difference between the $3t_2$ and the $2t_2$ orbitals (3.9 eV) is greater than measured (2.4 eV). Nevertheless, the ordering of the orbitals in the B_4Cl_4 INDO calculation is in complete accord with the STO-3G results and with those obtained in previous studies.[15,16]

The basic features in the spectra of B_8Cl_8 and B_9Cl_9, Figures 2 and 3, are similar to those found in the spectrum of B_4Cl_4. However, in B_4Cl_4 the ionization potentials of only 15 orbitals are within the energy regime shown in Figure 1. Symmetry considerations dictate that six bands occur; all are clearly resolved. In B_8Cl_8 and B_9Cl_9, because of the increase in size and the reduction in molecular symmetry, there are not only more orbitals in the same energy region (28 and 32, respectively) but also many more potentially distinct bands in each spectrum (21 in each case). This increase in size coupled with the reduction in symmetry results in many B_8Cl_8 and B_9Cl_9 orbitals which are very similar to one another in makeup and energy. It is this near degeneracy which accounts for the greater breadth of some of the B_8Cl_8 and B_9Cl_9 photoelectron envelopes (e.g., those near 12.3 eV), in comparison to the bands of B_4Cl_4. The incomplete resolution prevents the assignment of the B_8Cl_8 and B_9Cl_9 bands within the broad photoelectron envelopes. However, the calculations, including the population analysis, do allow the great majority of the orbitals to be assigned to the appropriate envelope; see Figures 2 and 3.

Assignment of the B_8Cl_8 Spectrum. The photoelectron spectrum of B_8Cl_8 can be assigned by either of two independent methods. The first relies upon the relatively accurate valence orbital ionization energies provided by the ab initio calculations. These values fall naturally into four groups as shown in Figure 4, the energy level diagrams for B_4Cl_4 and B_8Cl_8 obtained from the STO-3G ionization potentials contained in Tables I and II. Each of the B_8Cl_8 groups of orbitals corresponds to one of the photoelectron envelopes found in the spectrum. The population analysis (Table II) of each orbital within a given grouping of orbitals is similar to that of the other orbitals within the group but considerably different than that of the orbitals which contribute to an adjacent envelope of the spectrum.

The first group contains the $3b_1$, 10e, and $8a_1$ orbitals. They give rise to the envelope which maximizes at 10.69 eV (calculated 9.6–10.6 eV); see Figure 2 and Table II. The calculations indicate that these orbitals have mostly Cl 3p (63.8–69.5%) and B 2p (20.6–31.7%) character.

The second highest occupied group of orbitals includes the 9e, $7b_2$, 8e, $7a_1$, $2a_2$, $2b_1$, 7e, and $1a_2$ orbitals. These orbitals contribute to the envelope which is found at 12.16 eV (calculated 12.2–13.5 eV). They have the highest Cl 3p (83.9–91.0%) and the lowest B 2p (1.1–5.7%) components of all the orbitals of B_8Cl_8. Of the four energy regions considered for this molecule, the second contains the largest number of orbitals; in the spectrum of B_8Cl_8 the emission intensity of the envelope at 12.16 eV is greater than at any other energy.

The third group of orbitals contains the $6b_2$, 6e, $6a_1$, and 5e orbitals. The bands from these orbitals have been assigned to the envelope centered between 13.61 and 14.10 eV (calculated 14.1–14.9 eV). The STO-3G calculations indicate that this group is generally of higher B 2p (10.8–23.2%) and lower Cl 3p (60.1–80.8%) contribution than the orbitals of the second region.

The fourth group consists of the $1b_1$, $5b_2$, $4b_2$, $5a_1$, 4e, and $4a_1$ orbitals. These orbitals are assigned to the envelope of highest observed ionization potential, the one which maximizes at 15.58 eV (calculated 15.4–17.5 eV). They have the lowest Cl 3p (32.8–53.8%) and, with the exception of the $1b_1$ orbital, the highest Cl 3s (14.4–23.5%) character of any of the orbitals examined here. The ionization potential of the next more tightly bound pair of orbitals in B_8Cl_8 (3e) is calculated to be 20.7 eV.

A similar, but alternative, method for assigning the B_8Cl_8 photoelectron spectrum makes use of the INDO calculation for B_8Cl_8 in conjunction with the results of the same type of calculation on B_4Cl_4. As shown in Figure 5, the INDO calculations predict that the orbital ionization potentials for B_8Cl_8 fall into three groups. Each of these groups corresponds to one or more of the orbitals of B_4Cl_4. Rather than form a fourth group, however, the calculated ionization potentials of the most tightly bound orbitals observed in the spectrum are found at six discrete values.

The first B_8Cl_8 group of orbitals is calculated to have ionization potentials slightly greater than the $4t_2$ orbitals of B_4Cl_4. Experimentally, the envelope maxima are found at 10.55 and 10.69 eV for B_4Cl_4 and B_8Cl_8, respectively. The next 11 orbitals are projected to be closely spaced in energy, with ionization potentials which range from slightly less than the $1t_1$ orbitals of B_4Cl_4 to almost that of the 1e orbitals. Comparison of Figures 1 and 2 indicates that these predictions are also in accord with experiment. The second photoelectron envelope maximizes at 12.16 eV and tails off to the high-energy side.

The third group of orbitals are calculated to have ionization potentials similar to that of the $3t_2$ orbitals of B_4Cl_4, the latter occurring at 13.56 eV in the spectrum of B_4Cl_4. The third group of orbitals in B_8Cl_8 is thus assigned to the envelope centered between 13.61 and 14.10 eV.

The INDO calculations predict that the six bands in the region of highest observed ionization potential should be much more spread out in energy than is observed. This error in the INDO results is similar to that which previously occurred in the B_4Cl_4 calculation where the difference in energy between the $3a_1$ and $2t_2$ orbitals was predicted to be much larger than found. Accordingly, the final group of orbitals in B_8Cl_8 are all assigned to the PES envelope at 15.58 eV.

Assignment of the B_9Cl_9 Spectrum. For B_9Cl_9, like B_8Cl_8, the INDO calculations predict that the orbital ionization potentials fall into three relatively compact groups, but again the fourth group is computed to be broader in energy than is experimentally observed; see Figure 5. The first group, containing the 9e′, 6e″, and $7a_1'$ orbitals, corresponds closely in both calculated ionization potential and population to the $4t_2$ orbitals of B_4Cl_4 and to the $3b_1$, 10e, and $8a_1$ orbitals of B_8Cl_8. They are readily assigned to the photoelectron envelope which is found at 10.66 eV. The second group, the 11 orbitals of B_9Cl_9, 8e′, $2a_2'$, 5e″, $1a_1''$, $5a_2''$, 7e′, and 4e″, are all calculated to contain 99 ± 1% Cl 3p character, and the ionization potentials of these orbitals are all computed to be within 0.3 eV of the ionization potential of the $1t_1$ orbitals of B_4Cl_4. These orbitals are all assigned to the region of highest photoelectron intensity in the spectrum, the envelope at 12.28 eV.

The third group of orbitals in B_9Cl_9, $4a_2''$, $1a_2'$, $6e'$, $6a_1'$, $3e''$, $3a_2''$, and $5e'$, have reduced Cl 3p character, 63–89%, increased boron 2p populations, 10–26%, and calculated ionization potentials of 14.5–16.0 eV. The experimental ionization potentials of the B_4Cl_4 $3t_2$ orbitals and the six B_8Cl_8 corresponding orbitals are all in the range 13.6–14.1 eV. By analogy, the third group of B_9Cl_9 orbitals has been assigned to the bands occurring at 13.2 and 13.5 eV and to the envelope at 14.1 eV.

The final group of orbitals observed for B_9Cl_9, $5a_1'$, $4e'$, $4a_1'$, and $2e''$, all have increased Cl 3s character, decreased Cl 3p character, and calculated ionization potentials in excess of 16.0 eV, like the corresponding orbitals of B_4Cl_4 and B_8Cl_8. These orbitals have been assigned to the envelope centered at 15.85 eV in the spectrum.

In B_4Cl_4 there are five valence orbitals ($2a_1$, $1t_2$, and $1a_1$) that are too deep in energy to probe by He I photoelectron spectroscopy. They are chiefly derived from the Cl 3s electrons and the a_1 cage orbital into which a small amount of ligand character has been mixed. In B_8Cl_8 and B_9Cl_9 there are 12 and 13 orbitals, respectively, which cannot be examined by He I spectroscopy.

Variation of the B_9Cl_9 Geometry. Because the crystallographic data for B_9Cl_9 are incomplete, the geometry is uncertain. The theoretical effect of varying the prism height while maintaining the D_{3h} point group was examined by decreasing the prism height from 2.08 to 1.81 Å, the latter corresponding to the prism height of $B_9H_9^{2-}$.[41] According to the INDO calculations, the largest shifts in energy among the 32 highest occupied molecular orbitals (those observed in the PES spectrum) are stabilizations of the 4e' and the $1a_2'$ orbitals by 0.6 and 0.7 eV, respectively, and destabilizations of the 6e'' and 2e'' orbitals by 0.4 and 1.0 eV, respectively. The decrease in the calculated ionization potential of the 6e'' orbitals in the second geometry is accompanied by a decrease in the Cl 3p character, from 86.1 to 80.7%, and an increase in the B 2p character, from 12.6 to 17.5%.

If the vapor-phase geometry of the B_9Cl_9 molecule should correspond more closely to the second structure, the decrease in prism height does change the ordering of several orbitals, including the 9e' and the 6e'' orbitals. The change in geometry, however, does not alter the photoelectron envelopes to which any of the orbitals have been assigned.

Average Core Overlap Population Calculation. In addition to affording orbital and total energies, molecular orbital calculations also generate bond overlap populations, the last a theoretical measure of the strength of the bonding between two atoms. In closo cluster compounds like the boron halides examined here, in addition to bonds directed toward the ligands, the atoms forming the core of the cluster are also bonded to each of their nearest neighbors in the cage. In order to examine the average strength of the bonding between one of the boron atoms and the remainder of the framework, the "average core overlap population" has been obtained.

The basic approach is an extension of the ideas originally proposed by Mulliken to three-dimensional compounds. The average core overlap population is calculated in three steps. The first step is the computation of the overlap population, n, over all occupied molecular orbitals for the interactions between each pair of core atoms (atoms k and l)

$$n(k,l) = \sum_{r_k}\sum_{s_l}\sum_{i} 2C_{r_k}C_{s_l}S_{r_k s_l}$$

where there are two electrons in molecular orbital i; r_k and s_l are the appropriate atomic orbitals of atoms k and l, respectively, in molecular orbital i. In this equation $C_{i_{r_k}}$ is the coefficient for atomic orbital r on atom k in molecular orbital i and $C_{i_{s_l}}$ is similarly defined for atom l. $S_{r_k s_l}$ is the overlap integral of these atomic orbitals. See eq 4, ref 42. The second step is the summation of the individual overlaps, $n(k,l)$, over all of the boron–boron bonds which generates the total core overlap population. The average core overlap population is then obtained by dividing the total core overlap population by the number of boron atoms contributing equally or nearly equally to the bonding. In the present approach all of the core atoms are treated equivalently. Calculations upon more assymetric species would, of course, require a more localized approach.

Table IV. Overlap Populations and Approximate Decomposition Temperatures for the Boron Halides

compd	N^a	interactions[b]	ACOP[c,d]	ACOP[c,e]	B–Cl[f]	thermal dec, °C
B_2Cl_4, D_{2h}	2	1	0.397		0.598	
B_2Cl_4, D_{2d}	2	1	0.401	0.416	0.592	75
B_4Cl_4, D_{4h}	4	1	0.674	0.819	0.573	*k*
B_4Cl_4, T_d	4	6	0.720	1.006	0.600	~160
B_8Cl_8[g]	8	28	0.812	1.179	0.600	
B_8Cl_8[h]	8	28	0.822	1.221	0.593	~160
$B_8Cl_8^{2-}$[h]	8	28	0.902	1.246	0.522	*k*
B_9Cl_9[i]	9	36		1.263		400
$B_9Cl_9^{2-}$[i]	9	36		1.260		*k*
$B_9Cl_9^{2-}$[j]	9	36		1.288		*k*

[a] Number of boron atoms. [b] Number of boron–boron interactions examined. [c] Average core overlap population (per boron atom). [d] From STO-3G calculations. [e] From INDO calculations. [f] Average two-electron B–Cl bond overlap populations from STO-3G calculations. [g] Structure from ref 36. [h] Structure from ref 37. [i] Structure from ref 38. [j] Structure from ref 38 but prism height decreased to 1.81 Å. [k] Species unknown or thermal stability unreported.

The results of this calculation for B_2Cl_4, B_4Cl_4 (in both tetrahedral and square-planar polytopes), B_8Cl_8, $B_8Cl_8^{2-}$, B_9Cl_9, and $B_9Cl_9^{2-}$ are presented in Table IV. In the D_{4h} geometry the B–B bond lengths in B_4Cl_4 were assumed to be 1.719 Å, while the B–Cl distances were taken to be 1.759 Å.

Discussion

Appearance of the Spectra. As shown in Figures 1–3, the similarity of the spectra obtained from B_4Cl_4, B_8Cl_8, and B_9Cl_9 is remarkable. In the latter two molecules there are over 3 times as many energetically discrete orbitals as there are in B_4Cl_4, yet all of the measured ionization potentials of B_8Cl_8 and B_9Cl_9 fall into the energy regions previously mapped out by B_4Cl_4. Clearly, the gross features of the He(I) photoelectron spectra arise from the fact that all of these compounds are closo clusters comprised of BCl units. in each of the clusters the interactions among the boron and chlorine atoms must be similar. As discussed below the interactions fall into four general types; each type of interaction results in one of the regions of photoelectron activity found in the spectra. The trends in the spectra which occur as the cluster size increases appear to foreshadow the type of band structure associated with the solid state.

Assignment of the Spectra. The basic approach taken here is patterned after that which has been employed in the assignments of the photoelectron spectra of large aromatic species, compounds in which delocalization is found in two rather than three dimensions.[24-27] Given the large number of orbitals examined, the semiempirical and ab initio calculations are in surprisingly good agreement in the assignment of the photoelectron spectrum of B_4Cl_4 and B_8Cl_8. Both calculations predict a close correspondence in population and energy between the orbitals of B_8Cl_8 and those of B_4Cl_4. Comparison of the B_4Cl_4 results indicates that the ionization potentials afforded by INDO are less accurate, but that the energetic ordering of the orbitals predicted by both calculations is identical. For B_8Cl_8, both calculations provide groupings of orbitals that assign the same orbitals to the same envelopes in the spectrum, as shown in Figures 4 and 5, but they disagree upon the ordering of some of the orbitals within these envelopes. The complexity of the B_8Cl_8 spectrum does not allow an evaluation of the discrepancies between the two types of calculations. The INDO results from B_9Cl_9 indicate that the types of orbitals observed in this cluster compound are very much like those found in B_4Cl_4 and B_8Cl_8. It is this correspondence which has permitted the assignment of the B_9Cl_9 spectrum.

Apart from the differences in the ionization potentials anticipated and the exact ordering of the orbitals within some of the

(41) Guggenberger, L. J. *Inorg. Chem.* **1968**, *7*, 2260.
(42) Mulliken, R. S. *J. Chem. Phys.* **1955**, *23*, 1833.

envelopes in the spectrum, the major difference between the ab initio and the INDO calculations is related to the energy gaps between the lowest lying orbitals observed in the spectra. The INDO calculations suggest that these orbitals span a much broader energy range than predicted by the STO-3G calculations or observed experimentally.

For B_8Cl_8, assuming that the same geometry prevails in the gas phase as reported for the solid state, the uncertainties in the assignments lie in the relative energies of some of the orbitals within the various envelopes and perhaps in the assignments of the $1a_2$ and $5b_2$ orbitals. Both calculations indicate that the ionization potential and the population of the $1a_2$ orbital is intermediate between those of the 7e and $6b_2$ orbitals which contribute to the second and third envelopes of photoelectron activity, respectively. In either calculation the predicted ionization potentials and the population analysis of the $1a_2$ orbital corresponds more closely to those of the 7e orbitals; thus the $1a_2$ orbital has been assigned to the envelope which maximizes at 12.16 eV. From the INDO results alone, the assignment of the $5b_2$ orbital is difficult, but as shown in Figure 5, the calculated ionization potential of the $5b_2$ orbital is greater than that of any orbital which has been assigned to the third region of photoelectron activity.

For B_9Cl_9, the spectral assignment has been carried out without ab initio results. Based upon the comparisons above, all electron ab initio results for B_9Cl_9 might be expected to indicate smaller ionization potentials, a different ordering of the orbitals within the envelopes, and less spread in the predicted ionization potentials for the orbitals which contribute to the photoelectron envelope located near 15.85 eV. Taken as a whole, however, the comparisons of the ab initio and the INDO calculations for B_4Cl_4 and B_8Cl_8 suggest that the INDO results from B_9Cl_9, or even those from larger molecules, species much too large for ab initio calculations, can be treated with some confidence if the results are utilized in conjunction with those obtained from similar, but smaller, clusters.

Back Bonding in the Polynuclear Boron Chlorides. Back bonding by means of interactions between filled Cl 3p and unoccupied B 2p atomic orbitals has long been suggested to influence the stability of the boron halides. Typically, the back-bonding molecular orbitals have been defined as those in which the ligand–cage interactions are of π character and in which there is significant contribution from both B 2p and Cl 3p atomic orbitals. The extent of back bonding in a given compound, however, has proven difficult to quantify for several reasons, some of them semantic.

The original definition of back bonding is derived from Pauling's valence bond formalism and refers to the extent to which the appropriate canonical resonance forms contribute to the B–Cl bonding; the effect is to increase the B–Cl bond strength relative to a hypothetical B–Cl bond in which only σ bonding was present.[9,11,16,43] However, the same terminology, back bonding, has also been employed in the context of assessing the extent to which the boron–boron (framework) bonding has been augmented by the occupation of the back-bonding orbitals in the boron halides.[10,12–14,23] The two definitions are not necessarily synonymous.

In very simple molecules like BCl_3, back bonding is easily demonstrated and evaluated since in this compound only one occupied molecular orbital, the $1a_2''$ orbital, contains any interaction of π symmetry between the boron atom and the ligands. As shown in Figure 6, the eigenvectors of the atomic components of this orbital are all parallel, the overlap is everywhere positive, and there is no overlap of σ character in this orbital. To the extent that π bonding does occur in BCl_3, it is confined to one molecular orbital, the $1a_2''$ orbital. This orbital enhances the B–Cl bond strength.

In compounds even slightly more complex than BCl_3, however, the situtation is much less amenable to an approach in which only one type of orbital is singled out for attention. Three additional complications occur in the polynuclear boron chlorides. Two of these can be demonstrated by the B_2Cl_4 STO-3G results. The

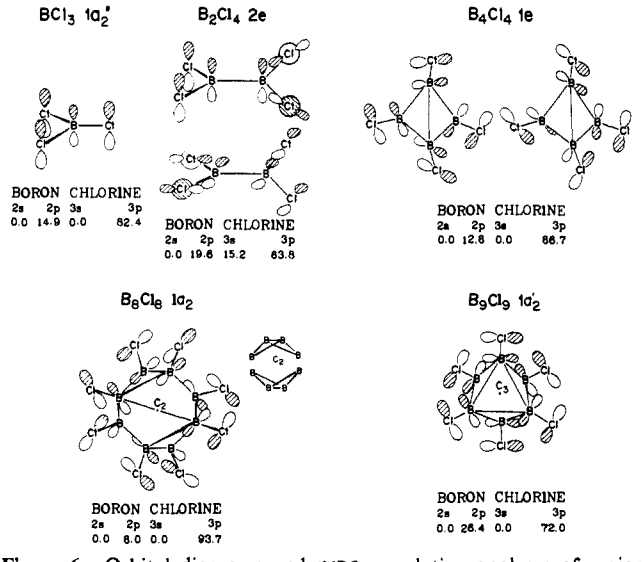

Figure 6. Orbital diagrams and INDO population analyses of major back-bonding orbitals in BCl_3 (r(B–Cl = 1.75 Å), B_2Cl_4, B_4Cl_4, B_8Cl_8, and B_9Cl_9. The B_8Cl_8 and B_9Cl_9 molecules are viewed along the C_2 and C_3 axes, respectively. In the B_9Cl_9 representation selected atoms and Cl 3p orbitals have been omitted for clarity.

first arises because the geometry of B_2Cl_4 is staggered in the gas phase.[33] No orbital is purely back bonding in character.

Although the 3e orbitals have been described as the back-bonding orbitals in B_2Cl_4,[43] these orbitals also contain interactions which are not of π character. In addition to interactions of local π symmetry between two of the chlorine atoms and the boron atom to which they are bonded, there are also interactions between the 2p orbital of the second boron atom and atomic hybrids from the second set of chlorine atoms; the latter are directed toward one or the other of the lobes of the second B 2p orbital. This is the mechanism by which Cl 3s but not B 2s character is admixed into the 2e and 3e orbitals of B_2Cl_4.[44] As shown in Figure 6, the B–Cl interactions in the 2e orbitals are similar. To evaluate the extent of back bonding in B_2Cl_4, it is necessary to examine several orbitals, but only part of each orbital, the part of local π symmetry, can be counted toward the net amount of back bonding which occurs.

The second complication occurring in B_2Cl_4 is a result of the node between the boron atoms in the 3e orbitals. The 3e orbitals increase the B–Cl bonding in B_2Cl_4, but they simultaneously decrease the boron–boron overlap. Depending upon the frame of reference then, the 3e orbitals of B_2Cl_4 are either back bonding (in part), because the π overlap strengthens the boron–chlorine bonds, or not back bonding, since the occupation of these orbitals weakens the boron–boron bond.

In all of the boron monochlorides, B_nCl_n, discussed here, symmetry does permit molecular orbitals which are solely B 2p and Cl 3p in makeup and in which the atomic components of the ligands are strictly in phase with those of the cage atoms. Some of these orbitals are also depicted in Figure 6. However, these are not the only orbitals that contribute to back bonding since in each compound there are also other orbitals in part of which the overlap is of π character. Like the 2e and 3e orbitals of B_2Cl_4, however, these other orbitals also contain regions which are not of local π symmetry.

A third feature not observed in BCl_3 is found in the boron monochlorides. In some of the molecular orbitals which are composed entirely of B 2p and Cl 3p atomic contributions, the boron–chlorine π overlap is antibonding. For example, if only the B_8 framework in B_8Cl_8 is considered, the B–B bonding gen-

(43) Lynaugh, N.; Lloyd, D. R.; Guest, M. F.; Hall, M. B.; Hillier, I. H. *J. Chem. Soc., Faraday Trans. 2* **1972**, *68*, 2192.

(44) The population analyses for the 2e and 3e orbitals of B_2Cl_4 from the STO-3G calculations are as follows. 2e orbitals: B_{2s}, 0.0%; B_{2p}, 16.5%; Cl_{3s}, 13.7%; Cl_{3p}, 64.0%. 3e orbital: B_{2s}, 0.0%; B_{2p}, 7.9%; Cl_{3s}, 0.6%; Cl_{3p}, 85.1%. The population analysis of the 2e orbitals obtained from the STO-3G calculations is very similar to the population analysis from the INDO calculations which is shown in Figure 6. Note that there is no node between the boron atoms in the 2e orbitals of B_2Cl_4.

erates two cage orbitals, of b_1 and a_2 symmetry, in which the boron–boron overlap is entirely B 2p in character. Both of these framework orbitals are bonding around the periphery of the two butterfly halves of the dodecahedron, but the lower energy b_1 cage orbital is bonding between the two halves of the cage, whereas the a_2 orbital is antibonding between the belt atoms; see Figure 6.

In molecular B_8Cl_8 the $1b_1$, $1a_2$, and $3b_1$ molecular orbitals are all filled; see Table II. In the $1b_1$ and the $1a_2$ orbitals, the boron 2p orbitals are all in phase with the 3p orbitals of the adjacent chlorine atoms. In the $3b_1$ orbital, however, while the overlaps are of π character, the overlap between the cage and the ligands is antibonding. This is because the molecular $1b_1$ and the $3b_1$ orbitals result from the bonding and antibonding combination of the b_1 framework orbital with the (tangential) chlorine 3p ligand group orbital of the same symmetry. Both orbitals increase the boron–boron overlap, but any enhancement of the B–Cl bonds due to π bonding in the $1b_1$ orbital has been offset by the occupation of the $3b_1$ orbital; see Table II.

The lowest unoccupied molecular orbitals of B_4Cl_4 (2e), $B_8Cl_8^{2-}$ ($3a_2$), and B_9Cl_9 ($3a_2'$) are similar to the $3b_1$ orbital of B_8Cl_8 in type. They are cage bonding, and the B–Cl interactions are all of π symmetry. The cage–ligand overlaps are all strictly antibonding. These orbitals, if occupied, would all enhance the boron–boron bond strengths, but they would also diminish the B–Cl bond strengths. They can be visualized by reversing the relative phases of the appropriate boron and chlorine orbitals in Figure 6.

Thus, by either interpretation of the term back bonding, in compounds larger than BCl_3 many orbitals contribute to back bonding—some positively, some negatively. In compounds larger than BCl_3, singling out one set of orbitals because of their symmetry is convenient but unproductive. Rather, the net contributions of all occupied molecular orbitals must be evaluated.

Average Core Overlap Population. One goal of this study has been to identify which cluster geometries are more stable than others by assessing the effectiveness of the framework bonding in different polytopes. The average core overlap population, the cluster analogue of the bond overlap population, is one potential gauge of the strength of the bonding by which an average boron atom is held to the rest of the framework.

The structural alternatives available to B_2Cl_4, which for the present purposes can be considered to be a dinuclear cluster, provide a convenient example of the utility of the overlap criteria. Here because there are two core (framework) atoms in the compound, the average core overlap population reduces to one-half of the two-electron boron–boron bond overlap population. Experimentally, the ground state of B_2Cl_4 in the gas phase has been determined to be the staggered D_{2d} configuration[33] rather than the eclipsed D_{2h} form found in the solid state.[32] The STO-3G calculations confirm that the D_{2d} rotamer is slightly more stable as the calculated total energy of the D_{2d} structure (−1867.200 au) is 2.6 kcal/mol lower in energy than that of the planar isomer.

Comparisons of the B–Cl bond overlap populations and the B–B bond overlap populations in Table IV indicate that in B_2Cl_4 the two geometries are nearly equivalent in energy because the increase in the boron–boron overlap which occurs upon rotation of the D_{2h} structure is offset by a decrease in the B–Cl bond overlap population. In the solid phase, the structure of B_2Cl_4 is determined by packing forces.[45]

In principle at least, the structure of B_4Cl_4 could be based upon either the square-planar or the tetrahedral polytope. In the former the boron–boron bonding would be expected to be of the two-center two-electron variety, whereas in the latter (real) geometry the boron–boron interactions are more delocalized. The STO-3G calculations indicate that the experimentally determined T_d structure (−1915.876 au) is 7.5 kcal/mol more stable than the D_{4h} structure presumed above.[46]

(45) Additionally, nonbonded repulsions are slightly lower in the D_{2d} structure, cf. ref 16. Electron diffraction data indicate a rotational barrier of 1.9 kcal/mol in the gas phase.[33]

Comparison of the average core overlap populations and the B–Cl bond overlap populations for the two B_4Cl_4 structures found in Table IV indicates that both the B–Cl and the B–B bonding is stronger in the tetrahedral geometry. They also suggest that the enhancement of the framework bonding may be the larger of the two effects.

The original crystallographic data obtained from B_8Cl_8 have been refined twice.[36,37] The calculated total energy of the second structure[37] (−3831.867 au) is 18.5 kcal/mol lower than the first. As shown in Table IV, the decrease in energy associated with the second structure results from better boron–boron bonding, accompanied by slightly poorer B–Cl bonding, the latter demonstrated by the decrease in the average B–Cl bond overlap population.

The addition of two electrons to the second structure, which generates the $2n + 2$ framework electron ion, $B_8Cl_8^{2-}$, does result in an increase in the average boron–boron overlap population, but a substantial decrease in the average B–Cl bond overlap population also occurs; see Table IV. Cluster reduction of B_8Cl_8 leads to stronger framework bonding but weaker ligand–framework bonds.

The INDO calculations indicate that the average core overlap population in $B_9Cl_9^{2-}$ is not larger than that found for B_9Cl_9 if the geometry assumed for the dianion is the same as that reported for the neutral compound. If the assumed prism height for $B_9Cl_9^{2-}$ is arbitrarily decreased from 2.08 Å to the 1.81 Å found for $B_9H_9^{2-}$, however, the average core overlap for the $2n + 2$ framework electron $B_9Cl_9^{2-}$ becomes larger than that for B_9Cl_9. This effect is not observed for B_8Cl_8. Curiously, the framework geometry found for B_8Cl_8 is very similar to that found in the borane dianion $B_8H_8^{2-}$.[47]

Because they are weak in comparison to the B–Cl bonds, the strength of the boron–boron bonding in the boron chlorides is expected to greatly influence the overall stability of these clusters. Since the bonding in all of the compounds is similar, the magnitude of the average core overlap population has been examined as a possible measure of the relative thermal stabilities. The average core overlap populations decrease in the order $B_9Cl_9^{2-}$ (prism height 1.81 Å) > B_9Cl_9 > $B_8Cl_8^{2-}$ > B_8Cl_8 > B_4Cl_4 (T_d) > B_4Cl_4 (D_{4h}) > B_2Cl_4 (D_{2d}) > B_2Cl_4 (D_{2h}). Note that where comparison is possible, the ab initio and the semiemperical calculations indicate the same trends for the average core overlap populations in the boron monochlorides. These trends correlate surprisingly well with thermal stability data for B_2Cl_4, B_4Cl_4, and B_9Cl_9. The correlation with B_8Cl_8 is less good; see Table IV.

Experimentally, B_4Cl_4 and B_8Cl_8 are of almost equal thermal stability, but B_4Cl_4 is more stable.[48] The average core overlap populations, however, are in the opposite order. The ACOP values, of course, presume that the clusters are well isolated from all external interactions including those of solvent. At the present time it is not clear whether the disagreement between the experimental thermal stabilities of B_8Cl_8 and B_4Cl_4 and the average core overlap populations arises from uncertainties in the calculations, unaccounted for effects of the solvent or other factors.

As yet the generality of the average core overlap population

(46) Utilizing a slightly different assumed geometry for square-planar B_4Cl_4, Lipscomb has shown that the inclusion of correlation corrections further increases the stability of the T_d polytope, relative to the D_{4h} structure, by as much as 51 kcal/mol. Mc Kee, M. L.; Lipscomb, W. N. *Inorg. Chem.* **1981**, *20*, 4148.

(47) Guggenberger, L. J. *Inorg. Chem.* **1969**, *8*, 2771.

(48) The hazards of comparing data obtained from thermal decomposition studies with the results from computational studies are well recognized. The chemical results are as follows: B_9Cl_9 is the most thermally and oxidatively stable of all of the polyhedral boron halides; it decomposes very slowly near 400 °C. Although B_4Cl_4 and B_8Cl_8 are of similar stability, in BCl_3 and CCl_4 solutions, B_4Cl_4 decomposes to a smaller extent than B_8Cl_8. In BCl_3 at 125 °C, 6% of the B_8Cl_8 (2 mol %) survives 70 h, whereas 42% of the B_4Cl_4 (1 mol %) was recovered after 72 h. In CCl_4, after 60 h at 160 °C, 9% of a sample of B_8Cl_8 (1 mol %) remained, while 92% of the B_4Cl_4 (1 mol %) was recovered. That solvent does play a role in these decompositions is clearly evident. The thermal stability of $B_9Cl_9^{2-}$ is unknown. The anion $B_8Cl_8^{2-}$ is unreported. The results obtained here suggest that the dianions $B_9Cl_9^{2-}$ and $B_8Cl_8^{2-}$ will be found to be more stable than the neutrals but that the $2n + 2$ framework electron $B_8Cl_8^{2-}$ ion may not be more stable than the neutral B_9Cl_9 molecule.

Table V. Highest Occupied Molecular Orbital Analyses

compd or ion	population anal B_{2s}	B_{2p}	Cl_{3s}	Cl_{3p}	H	HOMO symm	cage–ligand interaction[a]	calculation
B_4H_4[b]	8.5	56.0			35.0	$2t_2$	b	STO-3G
B_4Cl_4	12.1	25.4	0.0	57.6		$4t_2$	a	STO-3G
B_8H_8[c]	0.0	100.0			0.0	$1b_1$		STO-3G
B_8Cl_8[d]	0.0	31.7	0.0	63.8		$3b_1$	a	STO-3G
B_9H_9[e]	0.4	67.9			31.7	$4e'$	b	INDO/2
B_9Cl_9	0.5	12.9	0.0	85.7		$9e'$	a	INDO/2
$B_8H_8^{2-}$[f]	0.1	92.9			7.0	$4b_2$	b	STO-3G
$B_8Cl_8^{2-}$[d]	3.5	61.0	0.3	32.8		$8b_2$	a	STO-3G
$B_9H_9^{2-}$[g]	0.0	100.0			0.0	$1a_2'$		INDO/2
$B_9Cl_9^{2-}$[h,j]	0.0	55.3	0.0	39.1		$3a_2'$	a	INDO/2
$B_9Cl_9^{2-}$[i,j]	0.0	66.6	0.0	27.1		$3a_2'$	a	INDO/2

[a] b = bonding; a = antibonding. [b] Optimized T_d; B–H = 1.15 Å, B–B = 1.64 Å; also see ref 49. [c] Reference 46. [d] Reference 37; also see ref 50. [e] Reference 41; prism height increased to 2.08 Å. [f] Reference 46; see ref 51 also. [g] Reference 41. [h] Prism height, 2.08 Å. [i] Prism height, 1.81 Å. [j] Note that while a 14% decrease in the prism height does change the population analysis, it does not alter the conclusions.

method is not known. Experiments involving other core geometries, other core atoms, and different ligands are currently in progress.

Comparison of the Bonding of the Deltahedral Boron Hydrides with that of the Deltahedral Boron Chlorides. In the boron hydrides, B_nH_n, or their dianions, $B_nH_n^{2-}$, there are a total of $5n$ valence molecular orbitals of which only $2n$ or $2n + 1$ (ca. 40%) are occupied by electron pairs. The analogous chlorides, B_nCl_n, or their dianions, $B_nCl_n^{2-}$, differ in that there are $8n$ valence molecular orbitals of which $5n$ or $5n + 1$ (ca. 60%) are occupied.

One method for comparing the bonding in the two types of compounds is to envision positioning boron and hydrogen or boron and chlorine nuclei into the required closo geometries and then adding the appropriate number of valence electron pairs to the valence molecular orbitals in an aufbau type of approach. For the hypothetical neutral boron hydrides, B_nH_n, $2n$ pairs of electrons would be added. To the extent that the occupied molecular orbitals can be factored by type, as in the Hoffmann–Lipscomb approach,[49] the $2n$ pairs of electrons would form n B–H σ bonds and fill n of the $n + 1$ framework molecular orbitals.

To fill the corresponding molecular orbitals of the boron monochlorides, $3n$ pairs of electrons are required. If mixing between the molecular orbitals of different types were again prohibited, then the $3n$ pairs of electrons could be divided into n pairs to fill the molecular orbitals deepest in energy (which are derived from the Cl 3s electrons), n pairs for the molecular orbitals which bond the framework atoms together, and n pairs for the B–Cl σ bonds. The B–Cl bonds would employ the Cl 3p atomic orbitals directed toward the framework boron atoms.

Because only $3n$ pairs of valence electrons have been added at this point, the boron monochlorides would be cationic with a charge of $4n^+$. To form the neutral species, $2n$ more pairs of electrons are needed. They would enter molecular orbitals that are composed of the tangential chlorine 3p atomic orbitals, the 3p orbitals which are perpendicular to the boron–chlorine σ bonds. In the model above the last $2n$ pairs of electrons would be lone pairs.

The bonding in the real molecules is somewhat more complex, due to the effects of the various molecular point groups and, more importantly, due to the mixing of the different types of orbitals of the same symmetry. Qualitatively, however, the tangential Cl 3p orbitals are chiefly responsible for the three envelopes of lowest ionization potential observed in the photoelectron spectra, Figures 1–3. In each spectrum there is a band or envelope of bands located near 12.3 eV. These bands, as demonstrated by the population analyses in Tables I–III, arise from molecular orbitals in which the overlap between the cage and the chlorine atoms is minimal. They are pure Cl 3p lone pairs.

Flanking the bands from the lone pairs in the spectra are bands or envelopes of bands with ionization potentials near 10.6 and 13–14 eV. They are from orbitals in which the predominant interactions are the antibonding and bonding overlap of the perpendicular Cl 3p ligand group orbitals with the boron framework. Except for the $1b_1$ orbital of B_8Cl_8, discussed above, the fourth group of bands found in the spectra (near 15.7 eV) result from molecular orbitals in which B–Cl σ bonding predominates.

As indicated by the calculated ionization potentials listed in Tables I–III, until half of the valence molecular orbitals of the boron chlorides are filled [the $1t_1$ (B_4Cl_4), 8e (B_8Cl_8), and 5e″ (B_9Cl_9) orbitals] all of the interactions between the cage and the ligands are either bonding or nonbonding. But as the number of valence electron pairs increases from $4n$ to the $5n$ required for the neutral boron monochlorides, the valence molecular orbitals become more than half filled. Antibonding interactions between the cage and the ligands are observed. The final molecular orbitals filled in the boron chlorides are bonding, but less so than the molecular orbitals which are purely Cl 3p in composition; see Figures 1–3. The effect of adding the final n pairs of electrons to the boron monohalides is to offset some, but only some, of the earlier gains in bond strength arising from the positive overlap of the perpendicular Cl 3p atomic orbitals with the framework orbitals. Relative to the hydrides in which no ligand cage interactions of π symmetry occur, there is a net gain in energy due to the presence of the tangential Cl 3p atomic orbitals on the chlorine atoms in the boron chlorides.

The difference in bonding between the neutral boron hydrides and the neutral boron chlorides can be largely attributed to two factors. The first is related to the differences in σ bonding capability of the two types of ligand. The second is the net effect of the overlaps of the perpendicular Cl 3p orbitals with the cage. Together these factors result in stronger bonding in the chloride clusters than that in the hydrides. Experimentally, the neutral boron chlorides are well-known and relatively thermally stable, whereas none of the corresponding hydrides has yet been isolated. Calculations on B_4H_4, B_8H_8, and B_9H_9, such as those described below, do not suggest that the neutral boron hydrides are inherently unstable, but they do suggest that one of the reasons that, e.g., B_8H_8 and B_9H_9 have not been isolated to date is that these species might be much more prone to cluster reduction than B_8Cl_8 and B_9Cl_9 because of the differences in the composition of the highest occupied molecular orbitals in the two types of dianion.

Cluster Reduction. The reduction of the hypothetical neutral boron hydrides B_4H_4 and B_9H_9 would result in the occupation of the 1e and the $1a_2'$ orbitals, respectively. These orbitals are cage bonding; interaction between the framework and the ligands is symmetry forbidden. In B_8H_8, cluster reduction would result in the occupation of the $4b_2$ orbital. As shown in Table V, the $4b_2$ orbital is cage bonding and weakly cage–ligand bonding. In the hydrides, cluster reduction leads to the occupation of orbitals which are framework bonding; the interactions with the ligands in these orbitals are small or nonexistent. The effect of cluster reduction is to increase the boron–boron bond strength without greatly affecting the B–H bond strength. Although B_4H_4 may be too small

(49) Hoffmann, R.; Lipscomb, W. N. *J. Chem. Phys.* **1962**, *36*, 2179.
(50) Cox, D. N.; Mingos, D. M. P.; Hoffmann, R. *J. Chem. Soc., Dalton Trans.* **1981**, 1788.
(51) Kleier, D. A.; Lipscomb, W. N. *Inorg. Chem.* **1979**, *18*, 1312.

to support the charge required to completely fill the 1e orbitals, the $2n + 2$ framework electron borane dianions $B_8H_8^{2-}$ and $B_9H_9^{2-}$ are well-known and readily prepared.[41,47]

For the chlorides, however, the situation differs because of the contributions of the tangential chlorine 3p atomic orbitals. The reduction of the neutral species, B_nCl_n, would result in the occupation of the 2e (B_4Cl_4), $8b_2$ (B_8Cl_8), and $3a_2'$ (B_9Cl_9) orbitals. These orbitals correspond to the orbitals of the hydride anions in symmetry, but in the highest occupied $B_8Cl_8^{2-}$ and $B_9Cl_9^{2-}$ orbitals there is also a significant contribution that is derived from the Cl ligand group orbitals; see Table V. In each case this component is antibonding with respect to the boron framework. In the boron halide dianions, the occupation of the HOMO orbitals increases the boron-boron bond strength, but it simultaneously weakens the B-Cl bonding; see Table IV.

Examination of the core overlap population of the $1a_2'$ (HOMO) orbital of $B_9H_9^{2-}$ obtained from the INDO calculations confirms that this orbital is strongly boron-boron bonding; the average core overlap population in this orbital is +0.081. The B-H overlap in the $1a_2'$ orbital is, of course, 0; see Table V. For $B_9Cl_9^{2-}$ (prism height 1.81 Å), however, the INDO results indicate that the average B-Cl bond overlap population in the $3a_2'$ (HOMO) orbital is negative, -0.010. The average core overlap population in this orbital is positive, but only 0.047.

Thus the Hoffmann-Lipscomb approach,[49] which involves separating intracage from ligand-cage interactions, and the framework electron counting schemes, which explicitly or implicitly utilize this type of factorization, are successful in the borane dianions $B_8H_8^{2-}$ and $B_9H_9^{2-}$ because the highest occupied molecular orbitals in these species are totally framework bonding. These frontier orbitals are in fact best described as the $(n + 1)^{th}$ framework bonding molecular orbitals; see Table V. Neutral B_8H_8 and B_9H_9, if formed, would be expected to be exceptionally electrophilic.

In the boron chlorides, however, the framework electron counting rules are less successful because the underlying approximation is less valid. This is due to the antibonding contributions of the tangential Cl 3p atomic orbitals. The genesis of the antibonding overlaps is that well over half of the available molecular orbitals are filled. The practical result of the differences in the bonding between the two types of cluster is that B_8Cl_8 and B_9Cl_9 are less electrophilic than the analogous hydrides. For the chlorides both the neutral and the 2- oxidation states are chemically accessible. For the hydrides only the 2- clusters, $B_8H_8^{2-}$ and $B_9H_9^{2-}$, have been isolated to date.

Acknowledgment. We thank Prof. Michael Zerner (University of Florida) for providing the enlarged INDO program required for the B_8Cl_8 and B_9Cl_9 calculations. Support of this work by the National Institutes of Health, the National Science Foundation, the donors of Petroleum Research Fund, administered by the American Chemical Society, The American Cancer Society and the Computer Center of the University of Illinois at Chicago is gratefully acknowledged.

Electron Density Analysis of the Reaction of Aldehydes with Lithium Hydride. The General Importance of the HOMO-HOMO Interaction

Steven M. Bachrach and Andrew Streitwieser, Jr.*

Contribution from the Department of Chemistry, University of California, Berkeley, Berkeley, California 94720. *Received August 12, 1985*

Abstract: The transition states for the reactions of formaldehyde and acetaldehyde with lithium hydride were calculated at the restricted SCF level by using the 3-21G* basis set. Integrated electron population analysis indicates that lithium carries a charge of +0.85 in the transition state, nearly the same as in ground-state organolithium compounds. Molecular orbital analysis of these transition states reveals their HOMOs to be formed from both HOMO-LUMO and HOMO-HOMO interactions. The general importance of the HOMO-HOMO interaction is also shown through analysis of the transition state of the 1,3-cycloaddition of HCNO with acetylene.

Many theoretical studies of ground-state organolithium compounds have been reported in the recent literature. These studies indicate that the carbon-lithium bond is primarily ionic with only a small covalent component.[1] Coulomb's law alone reasonably predicts and explains the large number of experimentally and theoretically determined organolithium structures. We now turn to other states to see if ionicity remains dominant; in particular, does lithium act as a full cation in the transition state of a reaction involving organolithium compounds? Recent theoretical[2] and computational[3] advances have provided the opportunity to fairly readily calculate transition-state geometries. This report focuses on the electronic description of lithium compounds during the course of a reaction with emphasis on the transition state. In particular, we investigate the 1,2-addition of an organolithium reagent to a carbonyl by examining the prototypical reaction—lithium hydride addition to formaldehyde to form lithium methoxide (eq 1). Furthermore, molecular orbital analysis of the transition state points out a fundamental error inherent in many frontier molecular orbital applications.

$$H_2CO + LiH \rightarrow H_3COLi \quad (1)$$

Computational Methods

The calculations reported in this work were carried out by using the GAUSSIAN-82[3] package on a VAX-11/750. All structures were optimized at the restricted SCF level by using the 3-21G* basis set.[4] The transition

(1) For reviews, see: (a) Schleyer, P. v. R. *Pure Appl. Chem.* **1984**, *56*, 151. (b) Bachrach, S. M.; Streitwieser, A., Jr.; Schleyer, P. v. R., unpublished results.

(2) (a) Pople, J. A.; Krishnan, R.; Schlegel, H. B.; Binkley, J. S. *Int. J. Quantum Chem.* **1979**, *S13*, 225. (b) Saxe, P.; Yamaguchi, Y.; Schaefer, H. F., III *J. Chem. Phys.* **1982**, *77*, 5647. (c) Cerjan, C. J.; Miller, W. H. *J. Chem. Phys.* **1981**, *75*, 2800.

(3) Binkley, J. S.; Frisch, M. J.; DeFrees, D. J.; Raghavachari, K.; Whiteside, R. A.; Schlegel, H. B.; Fluder, E. M.; Pople, J. A., unpublished results, Carnegee-Mellon University.

(4) Gordon, M. S.; Binkley, J. S.; Pople, J. A.; Pietro, W. J.; Hehre, W. J. *J. Am. Chem. Soc.* **1982**, *104*, 2797. Exponents for the polarization functions were $\alpha_d(C) = 0.75$, $\alpha_d(O) = 0.8$.

0002-7863/86/1508-3946$01.50/0